International Journal of Innovative Research and Scientific Studies, 8(11) 2025, pages: 437-446

IJIRSS
International Journal of Innovative Research & Scientific Studies

ISSN: 2617-6548

URL: www.ijirss.com

Determination of optimal geometric parameters for empty concentrator–diffuser augmented wind turbines using the whale optimization algorithm

Ngwarai Shambira[1*], Patrick Mukumba[1] Golden Makaka[1]

[1]*Department of Computational Sciences, Faculty of Science & Agriculture, University of Fort Hare, Alice 5700, South Africa.*

Corresponding author: Ngwarai Shambira (*Email: nshambira@ufh.ac.za*)

Abstract

Expanding electricity access in off-grid regions, alongside increasing global energy demand, requires sustainable alternatives to fossil fuels, which are major drivers of greenhouse gas emissions. Wind energy provides a clean option but often suffers from intermittency and insufficient speeds in many locations, limiting turbine performance. This research focuses on improving energy capture in low-wind-speed areas, through an empty concentrator–diffuser augmented wind turbine (CDaugWT). A mathematical relationship linking throat velocity amplification to six geometric variables was developed, and these parameters were refined using the whale optimization algorithm (WOA), an artificial intelligence-based search technique. The final configuration achieved a maximum throat wind speed increase of 1.978 times. WOA outputs were in close agreement with those from response surface optimization, differing by just 1.3%. The optimum design included a diffuser angle of 10.5°, concentrator angle of 20.5°, concentrator length of 397.9 mm (0.66 Rth), diffuser length of 997.9 mm (1.65 Rth), throat length of 74.6 mm (0.12 Rth), and flange height of 104.6 mm (0.17 Rth), with Rth denoting the throat radius. Computational fluid dynamics validation showed only a 1.66 % deviation, confirming the robustness of the optimized design for enhancing wind turbine operation in resource-constrained environments.

Keywords: Concentrator-diffuser-augmented wind turbine, Shrouded wind turbines, Whale optimization algorithm, Wind energy.

DOI: 10.53894/ijirss.v8i11.10948
Funding: This study received no specific financial support.
History: Received: 30 September 2025 / **Revised:** 12 November 2025 / **Accepted:** 14 November 2025 / **Published:** 25 November 2025

Competing Interests: The authors declare that they have no competing interests.
Authors' Contributions: All authors contributed equally to the conception and design of the study. All authors have read and agreed to the published version of the manuscript.
Transparency: The authors confirm that the manuscript is an honest, accurate, and transparent account of the study; that no vital features of the study have been omitted; and that any discrepancies from the study as planned have been explained. This study followed all ethical practices during writing.
Acknowledgements: Special acknowledgement to the National Research Foundation (NRF), the Department of Research, Partnership and Innovation (DRPI) at the University of Fort Hare, Research Niche Area (RNA), Renewable Energy—Wind, for their financial support.
Publisher: Innovative Research Publishing

1. Introduction

The increasing global demand for electricity, coupled with the urgent need to mitigate the effects of climate change, such as heat waves experienced in Cape town, South Africa, and cyclones experienced in Mozambique and parts of Manicaland province in Zimbabwe has intensified the shift towards renewable energy technologies [1]. Wind energy, with its scalability and low environmental footprint, is a key contributor to this shift, yet its performance in low-wind-speed regions often below 5 m/s remains a significant challenge [2]. Conventional horizontal-axis wind turbines are often inefficient under such conditions, prompting exploration of augmentation systems such as concentrators and diffusers [3]. Several recent studies have shown that wind turbine performance can be significantly enhanced using concentrators and diffusers [4-6]. Concentrators capture wind over a large area and accelerate it through a smaller exit, increasing the velocity at the rotor [7]. Diffusers create low-pressure regions behind the rotor, drawing more airflow and increasing rotor-plane velocity, while also reducing tip-speed losses, rotor size, and yaw sensitivity compared to open turbines [8, 9]. Combining both concentrators and diffusers has been observed to further increase rotor velocity beyond what either device achieves alone [10, 11].

The geometric parameters of augmentation systems, such as concentrators and diffusers, play a decisive role in determining aerodynamic efficiency [12, 13]. A concentrator's effectiveness depends largely on its angle and length [14-16] while diffuser performance is strongly influenced by its length and divergence angle [17-19]. Adding a flange can further amplify wind speed [20-22]. In CDaugWT design, the cylindrical enclosure's throat length significantly affects airflow and velocity, with each geometric parameter exerting varying influence on downstream vortices [23]. Also, Shambira, et al. [24] demonstrated, through computational fluid dynamics (CFD) coupled with response surface methodology (RSM), that parameters including concentrator angle and length, diffuser angle and length, throat length, and flange height collectively govern the velocity augmentation capability of an empty concentrator–diffuser augmented wind turbine (CDaugWT). Their findings showed that the interaction between concentrator and diffuser lengths has the greatest impact, with throat wind speeds reaching nearly twice the free stream velocity.

Building on these insights, RSM has been widely applied to develop predictive models linking geometric parameters to velocity augmentation, explicitly capturing their simultaneous interaction effects often neglected in many studies and providing computationally efficient fitness functions for design optimization. For instance, Taghinezhad, et al. [6] formulated two quadratic RSM models for average wind speed in the shroud throat and available power, with $R^2 > 0.99$. Similarly, Bouvant, et al. [25] formulated a comprehensive second-order regression model for the power coefficient (C_P) in their study on the performance of an Archimedes screw turbine (AST) with $R^2 = 0.94$. In another study Khalid, et al. [26] explored diffuser design for hydrokinetic turbines and developed an RSM model for estimating fluid velocity at the diffuser throat with $R^2 = 0.96$ whilst Koc and Yavuz [27] optimized concentrator-flap-wind turbine combinations for peak flow velocities within the turbine area, developing a model using response surface methodology with $R^2 = 0.91$.

Conventional optimization methods, such as response surface optimisation (RSO) and gradient-based algorithms, have been widely applied in aerodynamic optimization but may converge prematurely or miss global optima [28]. Recently, metaheuristic algorithms inspired by natural processes, such as genetic algorithms (GA), particle swarm optimization (PSO), and the whale optimization algorithm (WOA), have shown promise in solving nonlinear, multi-dimensional design problems in wind energy [29-31]. WOA, in particular, has been successfully applied in turbine blade shape design, yaw control strategies, and hybrid renewable energy system sizing. Despite these advances, there remains a lack of systematic studies applying WOA to optimize multiple geometric parameters of empty concentrator–diffuser-augmented wind turbine design, particularly targeting low-wind-speed conditions typical of off-grid rural regions. Moreover, most previous research focuses on either concentrators or diffusers alone, rather than integrated CDaugWT designs.

This study addresses these gaps by building on the velocity augmentation model developed by Shambira, et al. [24] which mathematically links throat wind speed to six key geometric parameters of a CDaugWT design with $R^2 = 0.98$. An RSM model derived from this relationship is employed as a computationally efficient fitness function within WOA to refine the design. The optimization process is further validated using computational fluid dynamics (CFD) simulations, providing a robust methodology for enhancing energy capture in low-wind-speed areas and supporting the wider deployment of small-scale wind energy systems in resource-constrained environments.

Section 2 presents the research methodology, detailing the geometry of the CDaugWT structure and the procedures followed. Section 3 discusses the main findings, and Section 4 gives a conclusion, recommendations, and future work.

2. Methodology

The research followed a systematic procedure to optimize the CDaugWT design geometry. A quadratic response surface model served as the fitness function, and the whale optimisation algorithm was applied to search for optimal parameter values. The optimisation outcomes were validated using computational fluid dynamics (CFD) simulations conducted in ANSYS Fluent 2022R1. Custom MATLAB scripts for implementing WOA were developed and executed in MATLAB R2021a. The methodology is presented in detail in Sections 2.1–2.4. In Section 2.4, the numerical methodology used in this study follows the approach presented in Shambira, et al. [24]. For brevity, only a summary is provided here, with further details available in reference [24].

2.1. Geometry and Parameters of the CDaugWT Design

The concentrator-diffuser system geometry was defined using six key parameters recognised through literature studies: diffuser angle (θ_d), concentrator angle (θ_c), concentrator length (L_c), diffuser length (L_d), throat length

(L_{th}), flange height (H_f) [32, 33]. All dimensions were normalised with respect to the throat radius (R_{th}) to allow generalisation of the results. Figure 1 illustrates the geometry of the CDaugWT design.

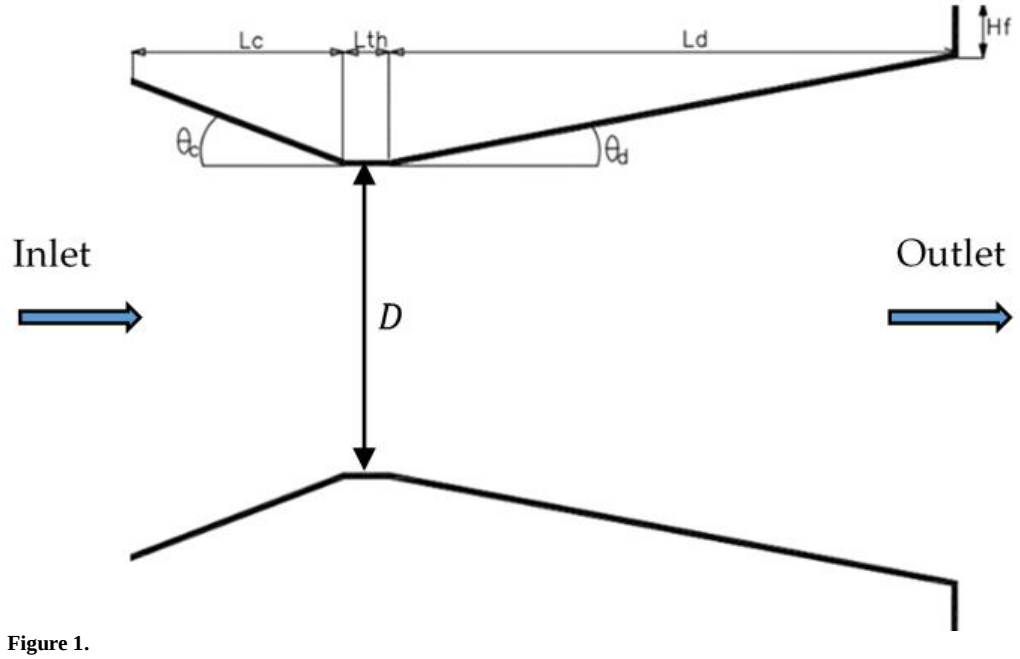

Figure 1.
Geometry of the CDaugWT Design.
Source: Shambira, et al. [24]

2.2. Fitness Function $\left(\frac{V_{th}}{V_\infty}\right)$

A velocity augmentation model was used as the fitness function. The goal was to maximize the velocity augmentation ratio, $V_r = \frac{V_{th}}{V_\infty}$, where V_{th} is the velocity at the throat, and V_∞ is the free stream velocity. This model, derived in Shambira, et al. [24] is a quadratic regression metamodel based on six geometric design parameters. It serves as the fitness function in a WOA used to optimise the concentrator-diffuser augmented wind turbine (CDaugWT) geometry for maximum wind speed augmentation. The fitness function is given as shown in Equation 1.

$$\frac{V_{th}}{V_\infty} = -0.752974 + 0.355948\,\theta_d + 0.280702\,\theta_c - 0.00431128\,L_c - 0.00217402\,L_d - 0.0133117\,L_{th} + 0.000363692\,H_f + 0.000214108\,(\theta_d \cdot L_c) + 4.976\times10^{-6}\,(L_c \cdot L_d) + 1.447\times10^{-5}\,(L_d \cdot L_{th}) - 0.0218753\theta_d^{\,2} - 0.00701959\,\theta_c^{\,2} - 3.20027\times10^{-6}\,L_c^{\,2}. \quad (1)$$

This study employs a throat wind speed estimation function to guide the WOA in maximizing velocity augmentation through CDaugWT geometry optimisation. Six continuous design parameters (1–6) define the optimisation space, each constrained within specific ranges as listed in Table 1. These parameters include the diffuser angle (θ_d), concentrator angle (θ_c), concentrator length (L_c), diffuser length (L_d), throat length (L_{th}), and flange height (H_f), all of which influence aerodynamic performance and are critical to achieving optimal flow conditions at the rotor plane. Since WOA is inherently a minimization algorithm, the fitness function was multiplied by –1 to enable maximization.

Table 1.
Design parameters ranges used in the study.

Parameter	Description	Range
1	Diffuser angle	$9.0° \leq \theta_d \leq 10.5°$
2	Concentrator angle	$19.0° \leq \theta_c \leq 20.5°$
3	Concentrator length	$327.10\text{ mm} \leq L_c \leq 397.90\text{ mm}$
4	Diffuser length	$927.10\text{ mm} \leq L_d \leq 997.90\text{ mm}$
5	Throat length	$60.40\text{ mm} \leq L_{th} \leq 74.60\text{ mm}$
6	Flange height	$90.40\text{ mm} \leq H_f \leq 104.60\text{ mm}$

2.3. Optimisation methodology

The whale optimization algorithm (WOA), proposed in 2016 by Mirjalili and Lewis [29] is a nature-inspired metaheuristic based on bubble-net feeding, which is a team-based eating method employed by groups of humpback whales. This algorithm mimics whales' strategy of creating multiple bubbles in a circle or nine-shaped paths to effectively capture prey [30, 34]. The foraging behavior of humpback whales is modelled in three main stages:

Step 1: Encircling the prey

The capacity of humpback whales to identify prey and encircle them is essential to the whale optimization method. In WOA, if ideal answer location is uncertain, current best represents target or is near optimum; agents update positions accordingly. As shown below, the procedure of surrounding the target can be mathematically represented:

$$\vec{D} = \left|\vec{C} \cdot \overrightarrow{X^*_{opt}}(t) - \overrightarrow{X_{ag}}(t)\right| \quad (2)$$

$$\overrightarrow{X_{ag}}(t+1) = \overrightarrow{X^*_{opt}}(t) - \vec{A} \cdot \vec{D} \quad (3)$$

where $\overrightarrow{X^*_{opt}}$ is the best solution (optimal CDaugWT geometry), $\overrightarrow{X_{ag}}$ denotes agent's position vector, while t represents the present iteration. The determination of the coefficient values for vectors $\vec{A}$ and $\vec{C}$ is shown below.

$$\vec{A} = 2\overrightarrow{a_d} \cdot \overrightarrow{r_{ran}} - \overrightarrow{a_d} \quad (4)$$

$$\vec{C} = 2\overrightarrow{r_{ran}} \quad (5)$$

with a_d decreasing linearly from 2 to 0 over iterations, and r_{ran} a random vector in [0,1]

Step 2: Algorithm of bubble net attacking (BNA)

This stage combines two strategies with equal probability as outlined below:

(i) Shrinking encircling mechanism

This strategy involves reducing the value of the vector $\overrightarrow{a_d}$, which results in a narrower fluctuation range for the coefficient vector $\vec{A}$, between $-a_d$ and a_d. Constraining $\vec{A}$ between -1 and 1 or ensuring $|\vec{A}| < 1$, determines the search agent's new position within the original to the current optimal region.

(ii) Spiral updating position

The whale follows a helix-shaped path to attack the prey in this strategy. Mathematically, given as:

$$\overline{D'} = \left|\overrightarrow{X^*_{opt}}(t - \overrightarrow{X_{ag}}(t)\right| \quad (6)$$

$$\overrightarrow{X_{ag}}(t+1) = \overline{D'} \cdot e^{bl} \cdot \cos(2\pi l) + \overrightarrow{X_{ag}}(t) \quad (7)$$

where $\overline{D'}$ refers to the distance between the i^{th} whale and the target prey, which is the optimal solution attained. where the distance between the intended prey and the i^{th} whale is the best solution found is denoted by $\overline{D'}$. The variable l is a randomly chosen number within the range of -1 to 1. The value of b stays fixed, uniquely linked to the form of the logarithmic spiral.

It is essential to emphasize that attacking and encircling are the two strategies the humpback whale uses simultaneously to capture its prey. As a result, the algorithm considers that there is an equal chance that any of the two strategies will be chosen. Therefore, the model below may be used to depict the whales' new location.

$$\overrightarrow{X_{ag}}(t+1) = \begin{cases} \text{Equation (3)}, & p_{ran} < 0.5 \\ \text{Equation (7)}, & p_{ran} \geq 0.5 \end{cases} \quad (8)$$

Here, a probability between 0 and 1 is denoted by p_{ran}

Step 3: Searching for prey

Humpback whales engage in random searching for prey, taking into the locations of other whales in the vicinity. To motivate the whales (searchers) to split out and scout new regions in an effort to find better prey, a coefficient represented by $\vec{A}$, can be utilized. This coefficient is set to a value beyond ±1 indicated by $|A| > 1$. The updated position is established at this stage by choosing a randomly chosen search agent over the best one found. This is expressed as:

$$\vec{D} = \left|\vec{C} \cdot X_{\text{rand}}(t) - \vec{X}(t)\right| \quad (9)$$

$$\vec{X}(t+1) = X_{\text{rand}}(t) - \vec{A} \cdot \vec{D} \quad (10)$$

X_{rand} is the random position vector.

The following is a summary of the WOA:

- Establish required parameters and initialize population X_{randi} $(i = 1,2, \ldots \ldots, N)$ and coefficient vectors a_d, A, C, l and p_{ran}

- Determine each search agent's fitness and choose the top candidate X^*_{opt}
- Update coefficient vectors in (first bullet point) based on the defined equations.
- Determining the value of p_{ran} and selecting the suitable strategy for the search agents' locations can be updated in the manner described below:
  (A) If $p_{ran} < 0.5$, evaluate the $|A|$ value. (i) The position is updated if the value of |A| is less than 1. using Equation 3. (ii) In the event where $|A| \geq 1$, choose a random search agent, X_{rand} and use Equation 10 to update the location.
  (B) Otherwise, if $p_{ran} \geq 0.5$, update the position using Equation 7.
- Ensure all search agents are considered and make necessary adjustments.
- Determine each search agent's fitness.
- Save the best solution, X^*_{opt}
- Check the stopping criteria. If not met, proceed to Step 3; if met, give the best answer, X^*_{opt} along with the fitness score that goes with it.

Table 2 presents the parameter values employed in the WOA, all of which fall within the recommended ranges and Figure 2. depicts the WOA flow chart.

Table 2.
WOA parameter specifications.

Parameter	Typical range	Suggested value
Convergence threshold	1×10^{-4} to 1×10^{-6}	1×10^{-6}
Population size	5 to 50	50
Maximum number of iterations	50 to 300	200

Source: Wadi and Elmasry [30] **and** Shambira, et al. [31]

2.4. Numerical methodology

The numerical methodology for analyzing airflow through the CDaugWT follows the approach in Shambira, et al. [24]. CFD simulations were performed using ANSYS Fluent, solving the steady, incompressible Reynolds-Averaged Navier–Stokes (RANS) equations. The shear stress transport (SST) k-ω turbulence model, a hybrid of the k-ε and k-ω models selected for its balance between accuracy and computational efficiency, was employed to accurately capture both near-wall and far-field flow effects, including separation, vortex formation, and shear layers [35, 36]. Second-order upwind schemes were applied for the convection–diffusion terms, with a residual convergence criterion of 1×10^{-6} [37]. A 2D axisymmetric computational domain was defined with velocity inlet of 2 m/s, free atmospheric pressure boundary condition outlet, and no-slip walls conditions [38]. The mesh was carefully generated, incorporating inflation layers near walls, and validated through grid independence and mesh-quality analyses, ensuring stability and accuracy. This methodology provided a detailed understanding of velocity augmentation and was essential for validating optimisation results. Complete numerical procedures and solver settings and the results are available in Hesami and Nikseresht [23].

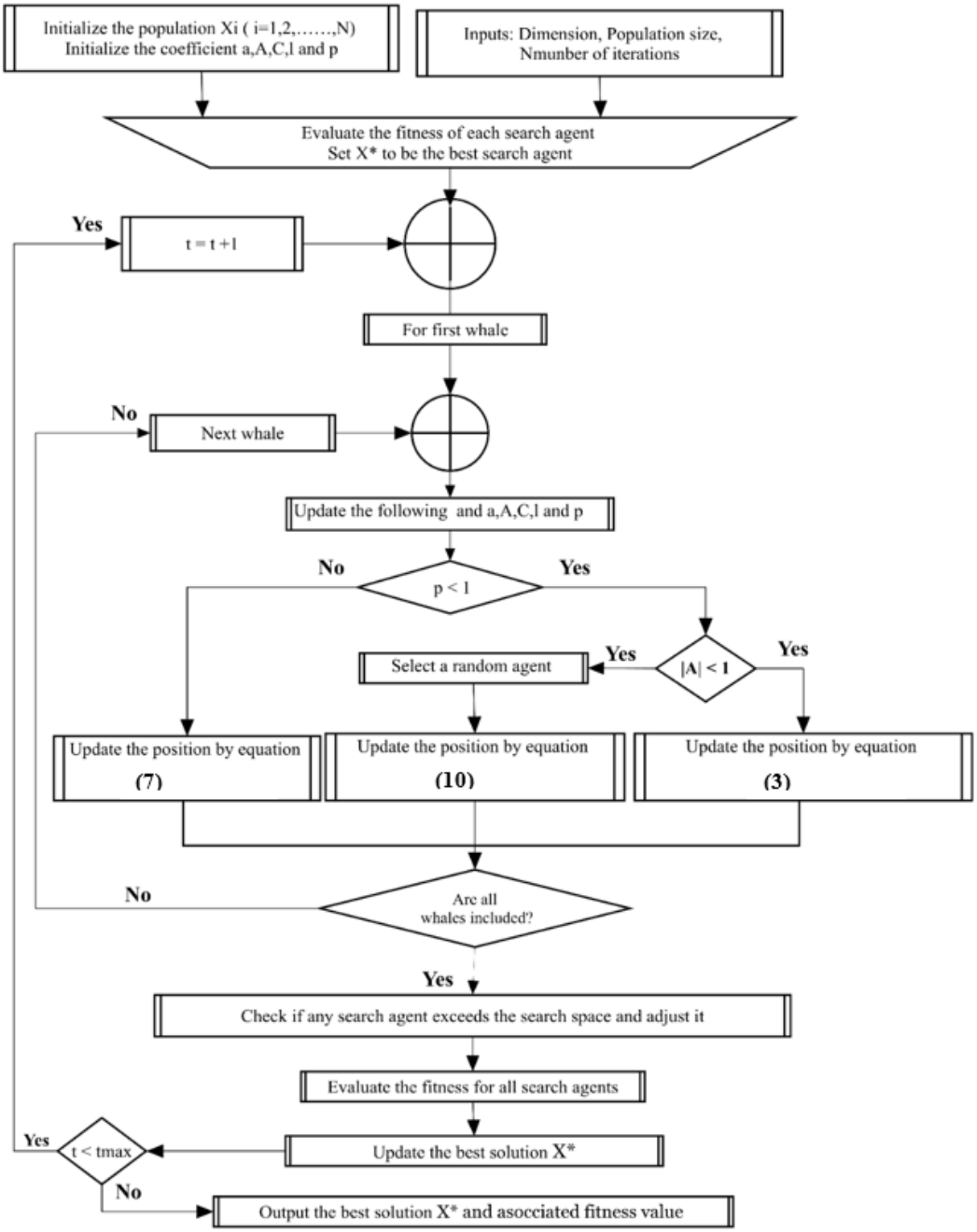

Figure 2.
Flow chart for whale optimization algorithm.
Source: Al-Mhairat and Al-Quraan [39]

3. Results and Discussion

3.1. Optimisation Results

The optimisation results in Table 3 show that WOA identified an optimal CDaugWT design with a diffuser angle (θ_d) of 10.5°, concentrator angle (θ_c) of 20.5°, concentrator length (L_c) of 397.9 mm ($0.66R_{th}$), diffuser length (L_d) of 997.9 mm ($1.65R_{th}$), throat length (L_{th}) of 74.6 mm ($0.12R_{th}$), and flange height (H_f) of 104.6 mm ($0.17\ R_{th}$). This configuration achieved a velocity augmentation ratio of 1.978, representing nearly a twofold increase in wind speed at the throat region compared to the free stream velocity.

The close agreement between optimisation methods and CFD validation, where WOA-predicted throat velocity was 1.3 % higher than RSM value and 1.66 % above CFD results, while RSM deviated from CFD by only 0.02%. These results demonstrate the robustness of the WOA in identifying near-optimal solutions. Comparable studies have highlighted the importance of precise diffuser and concentrator geometries in achieving such velocity gains. For example, Refaie, et al. [40] identified an optimal concentrator angle of 20° as a crucial component of the best concentrator configuration whilst Arifin, et al. [41] in their simulation results, found that diffuser angles between 8° and 16° had a better effect on wind turbine performance, with a power augmentation ratio of 1.6-2.1 times. Mann and Singh [42] showed that diffuser angles between 6° and 16° often provide an optimal balance between flow acceleration and avoiding separation. Similarly, the inclusion of a flange, as in the present design, has been reported to enhance flow entrainment and increase mass flow rate

through the rotor plane [4, 18]. Also, the optimal flange height obtained in this study maximizes airflow acceleration through the diffuser, ensuring effective vortex formation without causing excessive recirculation or structural issues, consistent with the findings of Hwang, et al. [43]. Additionally, the throat length was kept short to prevent flow separation while allowing adequate flow development before reaching the throat section, as noted in Taghinezhad, et al. [44].

The near-doubling of velocity within the throat is consistent with the findings of Rahmatian, et al. [5] who reported that convergent and divergent ducts can achieve velocity amplification ratios of up to 2.18, leading to substantial gains in power output due to the cubic relationship between wind speed and power. The optimised geometry here is therefore well positioned to extend operational capability into low-wind-speed regimes by lowering the cut-in speed, a known advantage of shrouded turbine configurations [2, 45, 46]. Figure 3 presents the 3D CDaugWT model in ANSYS Fluent based on these optimised parameters.

Table 3.
Optimised throat wind speed values validation with CFD results.

Method	θ_d	θ_c	$L_c(mm)$	L_d(mm)	L_{th}(mm)	H_f(mm)	$V_{th}(m/s)$	CFD $V_{th}(m/s)$	% Difference
RSM	10.0°	20.0°	375	975	70	100	3.906	3.8980	0.02
WOA	10.5°	20.5°	397.9	997.9	74.6	104.6	3.956	3.8908	1.66

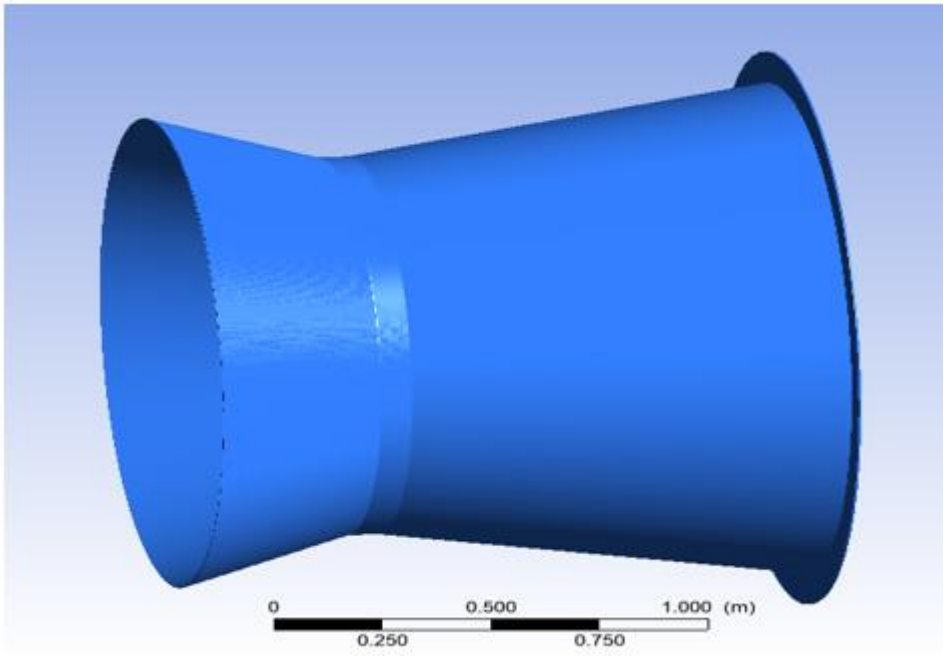

Figure 3.
The CDaugWT design.

3.2. CFD Analysis

The velocity contours in Figure 4 (top left) shows an increase in velocity at the structure's inlet (concentrator section), reaching its maximum at the throat (cylindrical section) where the wind turbine will be located. Subsequently, the velocity gradually decreases in the diffuser section, reaching its lowest value at the CDaugWT design outlet. This depicts a clear acceleration of the flow within the shroud throat region, where maximum wind speed is approximately 5.2 m/s. This acceleration indicates effective flow concentration by the shroud geometry, a direct outcome of the WOA-based optimization. Downstream, the velocity gradually recovers towards the free stream velocity value, of 2 m/s suggesting minimal wake losses.

Conversely, the pressure distribution illustrated in Figure 4 (top right) indicates a corresponding decrease in pressure at the structure's inlet, reaching its minimum of -14.2 Pa at the throat region. This localized low-pressure zone enhances the driving pressure gradient, effectively drawing more airflow through the turbine rotor plane. In the diffuser section (outlet), pressure gradually increases, returning to atmospheric pressure levels. The smooth recovery indicates favorable diffuser performance with minimal flow separation. Notably, the presence of a flange contributes to an additional pressure drop at the diffuser inlet, consistent with the findings of [4].

The axial distribution plots in Figure 4 (bottom) further quantifies these trends. The pressure profile along the x/R axis confirms a pronounced negative peak at the throat region x/R= 0, which corresponds to the region of maximum velocity. The velocity ratio profile (V_{th} / V_∞) peaks at approximately 2.6 in the same region, demonstrating a more than twofold increase in wind speed relative to the free stream velocity. These findings confirm that the WOA-optimised CDaugWT design geometry significantly amplifies local airflow velocity within the throat region, achieving more than double the free stream velocity. This acceleration effectively lowers the cut-in wind speed, allowing the turbine to begin operation under

lower wind conditions than would be possible with a conventional design [47]. As a result, the CDaugWT can operate for a greater portion of the year and maintain efficient performance even at wind speeds that would otherwise be insufficient to start a standard turbine [13, 45].

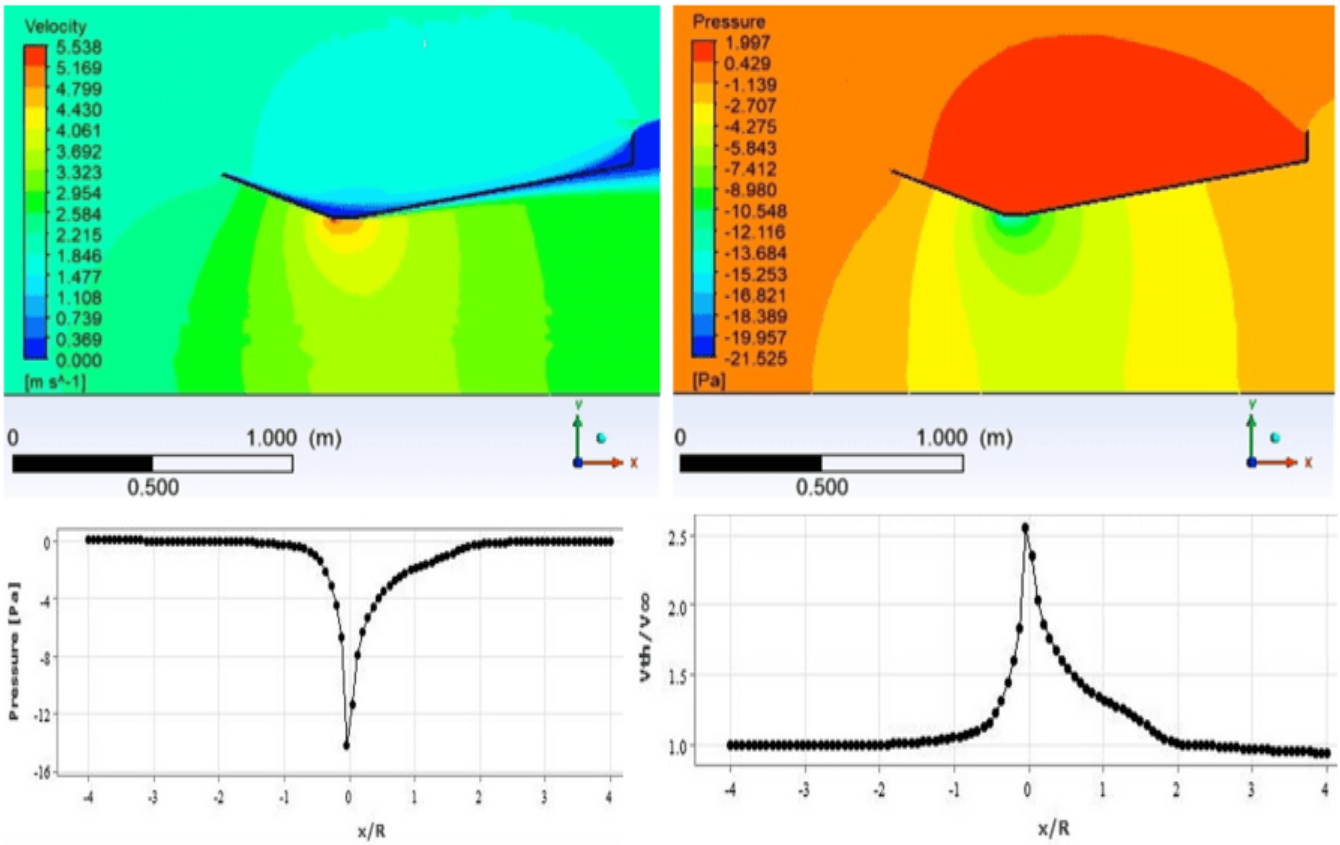

Figure 4.
Velocity, pressure contour distributions, and axial profiles for the CDaugWT design using the WOA.

4. Conclusion

This study demonstrates that applying the Whale Optimization Algorithm (WOA) to optimize the geometry of an empty concentrator–diffuser augmented wind turbine (CDaugWT) can substantially enhance wind turbine performance in low wind-speed regions. The optimal configuration, with $\theta_d = 10.5°$, $\theta_c = 20.5°$, $L_c = 0.66R_{th}$, $L_d = 1.65R_{th}$, $L_{th} = 0.12R_{th}$, and $H_f = 0.17R_{th}$, achieved a velocity augmentation ratio of 1.978, nearly doubling the throat wind speed relative to the free stream velocity. The WOA results showed strong agreement with both response surface methodology and computational fluid dynamics validations, confirming the reliability of the optimisation approach. The enhanced airflow through the shroud effectively lowers the cut-in wind speed, enabling turbines to operate in conditions that would otherwise be insufficient for conventional designs. These findings indicate that well-designed CDaugWT systems can extend the operational capabilities of small-scale wind turbines, increasing energy capture potential and making low-wind sites more viable for deployment.

Future research should involve field testing of the optimised CDaugWT design to validate simulation results and ensure accurate performance predictions and reliable applicability under real-world conditions. Multi-objective optimisation integrating structural integrity, cost, material efficiency, and durability is recommended to enhance practical deployment. As noted by Hosseini and Saboohi [48] holistic optimisation must balance aerodynamic efficiency, economic feasibility, and environmental suitability. Exploring alternative artificial intelligence optimisation methods such as particle swarm optimisation, grey wolf optimisation, and genetic algorithms could further improve convergence speed and design robustness. Additionally, extending this work to simulations with the turbine inside the optimised shroud would provide a more complete assessment of system performance.

References

[1] N. Shambira, P. Mukumba, and G. Makaka, "Assessing the wind energy potential: A case study in fort hare, south africa, using six statistical distribution models," *Applied Sciences*, vol. 15, no. 5, p. 2778, 2025. https://doi.org/10.3390/app15052778

[2] H. Hamid and R. M. Abd El Maksoud, "A numerical assessment of the heterogeneous effects of innovative shroud profiles for horizontal axis wind turbine," *Heliyon*, vol. 11, no. 2, p. e41661, 2025.

[3] N. Shambira, G. Makaka, and P. Mukumba, "Analytical models for concentrator and diffuser augmented wind turbines: A review," *International Journal of Smart Grid and Clean Energy (SGCE)*, vol. 10, pp. 123-132, 2021.

[4] H. S. A. Hameed, I. Hashem, M. A. Nawar, Y. A. Attai, and M. H. Mohamed, "Shape optimization of a shrouded Archimedean-spiral type wind turbine for small-scale applications," *Energy*, vol. 263, p. 125809, 2023.

[5] M. A. Rahmatian, A. Nazarian Shahrbabaki, and S. P. Moeini, "Single-objective optimization design of convergent-divergent ducts of ducted wind turbine using RSM and GA, to increase power coefficient of a small-scale horizontal axis wind turbine," *Energy*, vol. 269, p. 126822, 2023. https://doi.org/10.1016/j.energy.2023.126822

[6] J. Taghinezhad, S. Abdoli, V. Silva, S. Sheidaei, R. Alimardani, and E. Mahmoodi, "Computational fluid dynamic and response surface methodology coupling: A new method for optimization of the duct to be used in ducted wind turbines," *Heliyon*, vol. 9, no. 6, p. e17057, 2023.

[7] C. Shonhiwa, G. Makaka, P. Mukumba, and N. Shambira, "Determination of optimal geometry for an empty concentrator augmented wind turbine," *Physical Science International Journal*, vol. 27, pp. 75-90, 2023.

[8] S. Gujar, A. Auti, and S. Kale, "Advancements in wind energy: Exploring the potential of diffuser-augmented wind turbines (DAWTs)," *SSRG International Journal of Mechanical Engineering*, vol. 12, no. 1, pp. 12-23, 2025. https://doi.org/10.14445/23488360/IJME-V12I1P102

[9] E. S. Prakash, N. Madhukeshwara, V. G. Gunjalli, and D. Dadapeer, "Experimental investigation on a convergent-divergent shrouded small-scale wind turbine," *International Research Journal of Engineering and Technology*, vol. 2, no. 3, pp. 1745–1748, 2015.

[10] A. Manedeshmukh, S. Kulkarni, and S. Koli, "Experimentation of diffuser augmented wind turbine," *International Journal of Advance Research, Ideas and Innovations in Technology*, vol. 3, no. 2, pp. 864-867, 2017.

[11] S. A. Abdollahi, S. F. Ranjbar, M. Jafarai, M. B. Ehghaghi, and S. Faramarzi, "Enhancing wind energy efficiency: A study on the power output of shrouded wind turbines for a hydrogen storage system," *Results in Engineering*, vol. 26, p. 104710, 2025. https://doi.org/10.1016/j.rineng.2025.104710

[12] M. M. Naji and B. A. Jabbar, "Diffuser augmented wind turbine: A review study," *AIP Conference Proceedings*, vol. 3051, no. 1, p. 100015, 2024.

[13] A. Alkhabbaz, H.-S. Yang, W. Tongphong, and Y.-H. Lee, "Impact of compact diffuser shroud on wind turbine aerodynamic performance: CFD and experimental investigations," *International Journal of Mechanical Sciences*, vol. 216, p. 106978, 2022. https://doi.org/10.1016/j.ijmecsci.2021.106978

[14] S. Shikha, T. Bhatti, and D. Kothari, "Air concentrating nozzles: A promising option for wind turbines," *International Journal of Energy Technology and Policy*, vol. 3, no. 4, pp. 394-412, 2005. https://doi.org/10.1504/IJETP.2005.008403

[15] J. Orosa, E. García-Bustelo, and A. Oliveira, "An experimental test of low speed wind turbine concentrators," *Energy Sources, Part A: Recovery, Utilization, and Environmental Effects*, vol. 34, no. 13, pp. 1222-1230, 2012.

[16] S. Thangavelu, C. Goh, and C. Sia, "Design and flow simulation of concentrator augmented wind turbine," *IOP Conference Series: Materials Science and Engineering*, vol. 501, no. 1, p. 012041, 2019.

[17] M. I. Maulana, A. Syuhada, and M. Nawawi, "Analysis of diffuser augmented wind turbine (DAWT) with flange and curved interior using CFD," *AIP Conference Proceedings*, vol. 1984, no. 1, p. 020025, 2018.

[18] A. M. Elsayed, "Design optimization of diffuser augmented wind turbine," *CFD Letters*, vol. 13, no. 8, pp. 45-59, 2021.

[19] M. M. Takeyeldein, I. Ishak, and T. M. Lazim, "The effect of the number of the blades on diffuser augmented wind turbine performance," *Journal of Engineering Science and Technology*, vol. 18, no. 2, pp. 1019-1037, 2023.

[20] T. A. Jauhar, M. I. Hussain, T. Kiren, W. Arif, S. Miran, and G. H. Lee, "Effect of flanged diffuser divergence angle on wind turbine: A numerical investigation," *Plos one*, vol. 18, no. 6, p. e0287053, 2023. https://doi.org/10.1371/journal.pone.0287053

[21] Y. Y. Maw and M. T. Tun, "Sensitivity analysis of angle, length and brim height of the diffuser for the small diffuser augmented wind turbin," *ASEAN Engineering Journal*, vol. 11, no. 4, pp. 280-291, 2021.

[22] S. R. Hosseini and D. D. Ganji, "A novel design of nozzle-diffuser to enhance performance of INVELOX wind turbine," *Energy*, vol. 198, p. 117082, 2020.

[23] A. Hesami and A. H. Nikseresht, "Towards development and optimization of the Savonius wind turbine incorporated with a wind-lens," *Energy*, vol. 274, p. 127263, 2023.

[24] N. Shambira, G. Makaka, and P. Mukumba, "Velocity augmentation model for an empty concentrator-diffuser-augmented wind turbine and optimisation of geometrical parameters using surface response methodology," *Sustainability*, vol. 16, no. 4, p. 1707, 2024.

[25] M. Bouvant, J. Betancour, L. Velásquez, A. Rubio-Clemente, and E. Chica, "Design optimization of an Archimedes screw turbine for hydrokinetic applications using the response surface methodology," *Renewable Energy*, vol. 172, pp. 941-954, 2021. https://doi.org/10.1016/j.renene.2021.03.076

[26] W. Khalid, S. Sherbaz, A. Maqsood, and Z. Hussain, "Design and optimization of a diffuser for a horizontal axis hydrokinetic turbine using computational fluid dynamics based surrogate modelling," *Mechanics*, vol. 26, no. 2, pp. 161-170, 2020.

[27] E. Koc and T. Yavuz, "Effect of flap on the wind turbine-concentrator combination," *International Journal of Renewable Energy Resources*, vol. 9, no. 2, pp. 551-560, 2019.

[28] C. B. Allen, D. J. Poole, and T. C. S. Rendall, "Wing aerodynamic optimization using efficient mathematically-extracted modal design variables," *Optimization and Engineering*, vol. 19, no. 2, pp. 453-477, 2018. https://doi.org/10.1007/s11081-018-9376-7

[29] S. Mirjalili and A. Lewis, "The whale optimization algorithm," *Advances in Engineering Software*, vol. 95, pp. 51-67, 2016.

[30] M. Wadi and W. Elmasry, "A comparative assessment of five different distributions based on five different optimization methods for modeling wind speed distribution," *Gazi University Journal of Science*, vol. 36, no. 3, pp. 1096-1120, 2023.

[31] N. Shambira, L. Luvatsha, and P. Mukumba, "Comparative analysis of five numerical methods and the whale optimization algorithm for wind potential assessment: a case study in Whittlesea, Eastern Cape, South Africa," *Processes*, vol. 13, no. 5, p. 1344, 2025. https://doi.org/10.3390/pr13051344

[32] M. Aldhufairi, M. K. H. Muda, F. Mustapha, K. A. Ahmad, and N. Yidris, "Design of wind nozzle for nozzle augmented wind turbine," *Journal of Advanced Research in Fluid Mechanics and Thermal Sciences*, vol. 95, no. 1, pp. 36–43, 2022. https://doi.org/10.37934/arfmts.95.1.3643

[33] L. Ramayee, K. Supradeepan, P. Ravinder Reddy, and V. Karthik, "Design of shorter duct for wind turbines to enhance power generation: A numerical study," *Journal of the Brazilian Society of Mechanical Sciences and Engineering*, vol. 44, no. 4, p. 160, 2022.

[34] A. Al-Quraan, B. Al-Mhairat, A. M. Malkawi, A. Radaideh, and H. M. Al-Masri, "Optimal prediction of wind energy resources based on WOA—A case study in Jordan," *Sustainability*, vol. 15, no. 5, p. 3927, 2023.

[35] M. Anbarsooz and M. Amiri, "Towards enhancing the wind energy potential at the built environment: Geometry effects of two adjacent buildings," *Energy*, vol. 239, p. 122351, 2022.

[36] O. O. Ajayi, L. Unser, and J. O. Ojo, "Implicit rule for the application of the 2-parameters RANS turbulence models to solve flow problems around wind turbine rotor profiles," *Cleaner Engineering and Technology*, vol. 13, p. 100609, 2023. https://doi.org/10.1016/j.clet.2023.100609

[37] L. Ramayee and K. Supradeepan, "Influence of axial distance and duct angle in the improvement of power generation in duct augmented wind turbines," *Journal of Energy Resources Technology*, vol. 144, no. 9, p. 091302, 2022. https://doi.org/10.1115/1.4053615

[38] B. A. J. Al-Quraishi *et al.*, "CFD investigation of empty flanged diffuser augmented wind turbine," *International Journal of Integrated Engineering*, vol. 12, no. 3, pp. 22-32, 2020.

[39] B. Al-Mhairat and A. Al-Quraan, "Assessment of wind energy resources in Jordan using different optimization techniques," *Processes*, vol. 10, no. 1, p. 105, 2022.

[40] A. G. Refaie, H. S. A. Hameed, M. A. A. Nawar, Y. A. Attai, and M. H. Mohamed, "Comparative investigation of the aerodynamic performance for several Shrouded Archimedes Spiral Wind Turbines," *Energy*, vol. 239, p. 122295, 2022/01/15/ 2022. https://doi.org/10.1016/j.energy.2021.122295

[41] F. Arifin *et al.*, "Modelling design diffuser horizontal axis wind turbine," presented at the 5th FIRST T1 T2 2021 International Conference (FIRST-T1-T2 2021), 2022.

[42] H. S. Mann and P. K. Singh, "Energy recovery ducted turbine (ERDT) system for chimney flue gases - A CFD based analysis to study the effect of number of blade and diffuser angle," *Energy*, vol. 213, p. 118501, 2020. https://doi.org/10.1016/j.energy.2020.118501

[43] P.-W. Hwang, J.-H. Wu, and Y.-J. Chang, "Optimization based on computational fluid dynamics and machine learning for the performance of diffuser-augmented wind turbines with inlet shrouds," *Sustainability*, vol. 16, no. 9, p. 3648, 2024. https://doi.org/10.3390/su16093648

[44] J. Taghinezhad, R. Alimardani, M. Masdari, and H. Mosazadeh, "Parametric study and flow characteristics of a new duct for ducted wind turbines system using analytical hierarchy process: Numerical & experimental study," *Energy Systems*, vol. 15, no. 2, pp. 585-614, 2024.

[45] A. Aranake and K. Duraisamy, "Aerodynamic optimization of shrouded wind turbines," *Wind Energy*, vol. 20, no. 5, pp. 877-889, 2017.

[46] A. Saleem and M.-H. Kim, "Effect of rotor tip clearance on the aerodynamic performance of an aerofoil-based ducted wind turbine," *Energy Conversion and Management*, vol. 201, p. 112186, 2019. https://doi.org/10.1016/j.enconman.2019.112186

[47] M. Nasrul and I. Rizianiza, "Shrouded wind turbine for low wind speed," *IOP Conference Series: Materials Science and Engineering*, vol. 1034, no. 1, p. 012042, 2021.

[48] S. E. Hosseini and Z. Saboohi, "Ducted wind turbines: A review and assessment of different design models," *Wind Engineering*, vol. 49, no. 3, pp. 833-854, 2025. https://doi.org/10.1177/0309524X241282090